

Original Paper

Empagliflozin and Dapagliflozin Reduce ROS Generation and Restore NO Bioavailability in Tumor Necrosis Factor α -Stimulated Human Coronary Arterial Endothelial Cells

Laween Uthman^a Anna Homayr^{a,b} Rio P. Juni^c Eva L. Spin^a
Raphaella Kerindongo^a Marleen Boomsma^a Markus W. Hollmann^a
Benedikt Preckel^a Pieter Koolwijk^c Victor W.M. van Hinsbergh^c
Coert J. Zuurbier^a Martin Albrecht^b Nina C. Weber^a

^aDepartment of Anesthesiology, Laboratory of Experimental Intensive Care and Anesthesiology (L.E.I.C.A.), Amsterdam UMC, location Academic Medical Centre (AMC), University of Amsterdam, Amsterdam Cardiovascular Sciences, Amsterdam, the Netherlands, ^bDepartment of Anesthesiology and Intensive Care Medicine, UKSH, Campus Kiel, Kiel, Germany, ^cDepartment of Physiology, Amsterdam UMC, location VU medical center (VUMC), VU University, Amsterdam Cardiovascular Sciences, Amsterdam, the Netherlands

Key Words

SGLT2 inhibitors • Inflammation • Endothelial cell • Empagliflozin • TNF α

Abstract

Background/Aims: Heart failure is characterized by chronic low-grade vascular inflammation, which in itself can lead to endothelial dysfunction. Clinical trials showed reductions in heart failure-related hospitalizations of type 2 diabetic patients using sodium glucose co-transporter 2 inhibitors (SGLT2i's). Whether and how SGLT2i's directly affect the endothelium under inflammatory conditions is not completely understood. The aim of the study was to investigate whether the SGLT2i Empagliflozin (EMPA) and Dapagliflozin (DAPA) reduce tumor necrosis factor α (TNF α) induced endothelial inflammation *in vitro*. **Methods:** Human coronary arterial endothelial cells (HCAECs) and human umbilical vein endothelial cells (HUVECs) were (pre-)incubated with 1 μ M EMPA or DAPA and subsequently exposed to 10 ng/ml TNF α . ROS and NO were measured using live cell imaging. Target proteins were either determined by infrared western blotting or fluorescence activated cell sorting (FACS). The connection between Cav-1 and eNOS was determined by co-immunoprecipitation. **Results:** Nitric oxide (NO) bioavailability was reduced by TNF α and both EMPA and DAPA restored NO levels in TNF α -

L. Uthman and A. Homayr contributed equally to this manuscript.

Nina C. Weber

Department of Anesthesiology, Laboratory of Experimental Intensive Care and Anesthesiology (L.E.I.C.A.)
Amsterdam UMC, location Academic Medical Centre (AMC), Meibergdreef 9, Room M0-128, Amsterdam,
Noord-Holland, 1105 AZ (The Netherlands)
Tel. +31 20 5668215, E-Mail N.C.Hauck@amc.uva.nl

stimulated HCAECs. Intracellular ROS was increased by TNF α , and this increase was completely abolished by EMPA and DAPA in HCAECs by means of live cell imaging. eNOS signaling was significantly disturbed after 24 h when cells were exposed to TNF α for 24h, yet the presence of both SGLT2is did not prevent this disruption. TNF α -induced enhanced permeability at t=24h was unaffected in HUVECs by EMPA. Similarly, adhesion molecule expression (VCAM-1 and ICAM-1) was elevated after 4h TNF α (1.5-5.5 fold increase of VCAM-1 and 4-12 fold increase of ICAM-1) but were unaffected by EMPA and DAPA in both cell types. Although we detected expression of SGLT2 protein levels, the fact that we could not silence this expression by means of siRNA and the mRNA levels of SGLT2 were not detectable in HCAECs, suggests aspecificity or our SGLT2 antibody and absence of SGLT2 in our cells. **Conclusion:** These data suggest that EMPA and DAPA rather restore NO bioavailability by inhibiting ROS generation than by affecting eNOS expression or signaling, barrier function and adhesion molecules expression in TNF α -induced endothelial cells. Furthermore, the observed effects cannot be ascribed to the inhibition of SGLT2 in endothelial cells.

© 2019 The Author(s). Published by
Cell Physiol Biochem Press GmbH&Co. KG

Introduction

Type 2 diabetes (T2D) and heart failure have a bi-directional relationship, whereby the development and progression of one disease may impact the other. Both conditions promote a systemic pro-inflammatory state in the heart and vasculature. Insulin resistance has been associated with increased levels of circulating inflammatory factors, including tumor necrosis factor α (TNF α), which was linked to endothelial dysfunction [1]. TNF α , a 17 kDa cytokine, is released by different cell types, mainly leukocytes and other immune cells, as a response to systemic inflammation. TNF α signaling promotes endothelial dysfunction by negatively affecting NO bioavailability, endothelial nitric oxide synthase (eNOS) signaling, and increasing reactive oxygen species (ROS), permeability and adhesion molecules in the endothelium [2–6].

A novel class of glucose-lowering compounds targeting the kidney-specific sodium glucose co-transporter 2 (SGLT2) have been applied as a treatment strategy in T2D patients. Cardiovascular outcome trials show that empagliflozin (EMPA) effectively reduces cardiovascular-related death and that EMPA, dapagliflozin (DAPA) and canagliflozin (CANA) consistently reduce heart failure-related hospitalization in T2D patients [7–9]. The underlying mechanisms for the beneficial actions of SGLT2 inhibitors (SGLT2i's) remain unclear. *In vivo* studies suggest anti-inflammatory actions of SGLT2i's in the aortic valve, coronary microvascular endothelial cells, the kidney and the heart [10–14]. However, these *in vivo* results cannot discriminate between anti-inflammatory actions of SGLT2i's explained by systemic alterations or via a direct effect on cardiovascular cells. One of the first studies addressing direct anti-inflammatory effects of SGLT2i's reported moderate reductions in adhesion molecule expression in TNF α treated endothelial cells at certain concentrations of DAPA [15]. EMPA has been reported to restore cell viability and ATP content in endothelial cells exposed to hypoxia reoxygenation injury [16]. A recent study by Mancini et al. reported anti-inflammatory properties of the SGLT2i CANA in IL-1 β stimulated endothelial cells [17].

To date, the effects of the SGLT2i's EMPA and DAPA in TNF α -stimulated endothelial cells, especially different cardiac endothelial cells is not completely understood [18]. EMPA, DAPA and CANA appear to act differently on endothelial cells. Due to the contradictory results with regard to the direct effects of SGLT2i's in vascular inflammation [15, 17], it has been challenging to speculate on the direct endothelial cell effects of EMPA. Therefore, we aimed to examine whether the SGLT2i's EMPA and DAPA ameliorate endothelial function in TNF α -treated primary human endothelial cells. We hypothesized that EMPA and DAPA attenuate TNF α -induced endothelial inflammation through direct actions on endothelial cells.

Materials and Methods

Cell culture

HCAECs were purchased from ATCC (Manassas, VA, USA) and grown in vascular basal cell medium with supplements (ATCC), containing 5 ng/ml vascular endothelial growth factor, 5 ng/ml epidermal growth factor, 5 ng/ml fibroblastic growth factor, 15 ng/ml insulin-like growth factor 1, 10 mM L-glutamine, 0.75 U/ml heparin sulfate, 1 μ g/ml hydrocortisone, 50 μ g/ml ascorbic acid, 1% amphotericin B, 1% penicillin-streptomycin and 10% FBS (TICO).

The isolation of Human umbilical vein endothelial cells (HUVECs) from human umbilical cords has been waived by the medical ethical committee: W12-167#12.17.096 Amsterdam, the Netherlands. HUVECs were freshly isolated from human umbilical cords as described previously [19, 20]. HUVECs were grown in endothelial cell growth medium (Promocell, Heidelberg, Germany) supplemented with 10% heat-inactivated fetal bovine serum (FBS; TICO Europe, Amstelveen, Netherlands), 1% amphotericin B solution (Gibco, Paisley, UK) and 1% penicillin-streptomycin (Sigma-Aldrich, St. Louis, MO, USA). HUVECs purity was determined and confirmed (Supplementary Fig. 1 – for all supplemental material see www.cellphysiolbiochem.com) by flow cytometry analysis (FACS) of von Willebrand Factor (vWF) using Fluorescein (FITC)-labelled Anti-vWF antibody (Bio-Rad, Wiesbaden, Germany).

All cells were cultured in gelatin (0.75%) coated flasks and maintained in a humidified atmosphere of 5% carbon dioxide/95% air at 37°C (CO₂ Incubator Heracell 150i, Thermo Fisher Scientific, Waltham, MA, USA). Cultures were passaged by brief trypsinization using 0.05% Trypsin-EDTA (Gibco) and medium M199 (PAN biotech, Aidenbach, Germany) supplemented with 10% FBS, 1% amphotericin B, 1% penicillin-streptomycin and 1% L-glutamine. All experiments were initiated with HUVECs from passage 2 to 3 and HCAECs from passage 5 to 8 when they reached 80-90% confluency.

Before treatment, the cells were washed three times with phosphate buffered saline (PBS) and starved overnight by FBS reduction to 2% in the media. Experiments were carried out under three or four

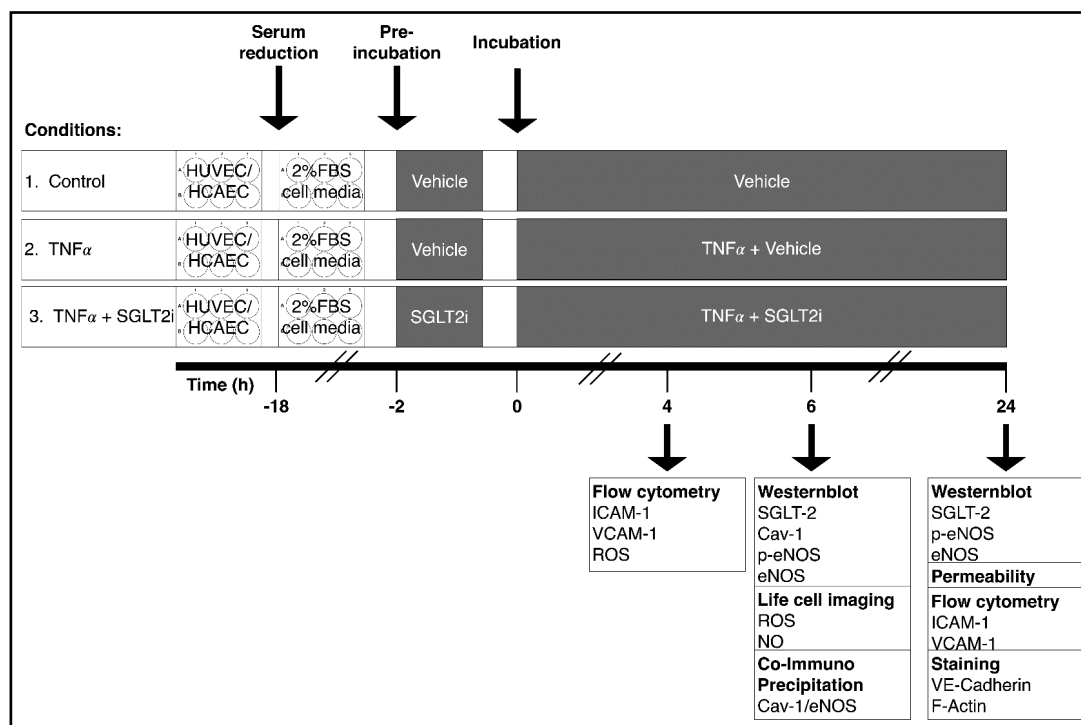


Fig. 1. Experimental protocol outline. Cells were starved by serum reduction for 16h before pre-incubation with an SGLT2i (1 μ M) or vehicle (0.02% DMSO) for 2h. Stimulation with 10 ng/ml TNF α occurred for 4–24h. Cells were treated for 4h for detection of adhesion molecules (ICAM-1, VCAM-1) and intracellular ROS levels, for 6h and 24h for western blot analysis, ROS and NO. Permeability and cell staining were assessed after 24h.

conditions: vehicle, EMPA alone, TNF α (10 ng/ml; Sigma Aldrich), and TNF α with SGLT2i treatment using EMPA (MedChem Express, NJ, USA). Since a previous study in TNF α stimulated HUVECs showed restored eNOS signaling and adhesion molecules expression in the presence of DAPA [15], DAPA (MedChem Express) was also investigated for several measurements. Thus, EMPA or DAPA 5 mM stock solutions dissolved in 100% DMSO was added in the medium to a final concentration of 1 μ M. Cells were pre-incubated with either EMPA, DAPA or vehicle (DMSO) containing media for 2 h. Subsequently, cells were treated with EMPA, DAPA or vehicle, either in the presence or absence of 10 ng/ml TNF α (Fig. 1).

Intracellular NO measurement

The measurement of nitric oxide level was performed as previously described [18]. In brief, exposure to 10ng/ml TNF α , 1 μ M EMPA or DAPA, and/or the combination thereof occurred for 6 h, during which the cells were incubated with copper-based NO probe (Cu2FL2E, 96-0396, Strem) for the final 45 min of treatment at a final concentration of 20 μ M. The cells were then washed, followed by live-cell imaging at 37°C and 5% CO₂ environment on a Zeiss Axiovert 200M Marianas inverted fluorescence microscope (Intelligent Imaging Innovations) with a 63X oil-immersion objective. All fluorescent images were corrected for background signals. Quantification of fluorescent images of HCAECs and HUVECs were performed using digital cell masking software (Slidebook 6, Intelligent Imaging Innovations) and ImageJ, respectively.

ROS detection – live cell imaging

The seeding of cells and measurement of ROS were conducted as described previously [18]. In brief, HCAECs were exposed to 10ng/ml TNF α , 1 μ M EMPA or DAPA, and/or the combination thereof for 6h, during which the cells were incubated with the fluorescent dye-based ROS probe for the last 30 min of treatment (CM-H2DCFDA, C6827, Thermo Fisher) at a final concentration of 5 μ M in PBS (220/12257974/1110, Braun). Washing the cells was followed by live-cell imaging at 37°C and 5% CO₂ environment on a Zeiss Axiovert 200M Marianas inverted fluorescence microscope (Intelligent Imaging Innovations, Denver, CO, USA) with a 63X oil-immersion objective. All fluorescent images were corrected for background and negative controls. Quantification of fluorescent images of HCAECs and HUVECs were performed using digital cell masking software (Slidebook 6, Intelligent Imaging Innovations) and ImageJ, respectively.

ROS detection – FACS assay

Intracellular ROS levels were also determined using ROS-ID Total ROS detection Kit (Enzo Lifescience Europe, Lausen, Switzerland) according to the supplier's instructions as described previously [21]. Briefly, cells were cultured in 6-well plates, harvested by brief trypsinization and centrifuged for 5 min at 31 g and 22 °C. The pellet was resuspended in the provided washing buffer. Cell number was counted and adjusted using Z2 coulter counter (Beckman Coulter, Brea, CA, USA). One million cells were stained with 0.125 μ M of detection reagent for 30 min at 37°C. Samples were kept in the dark at room temperature until analysis. Measurements were carried out using FACS Canto II (Becton Dickinson, Franklin Lakes, NJ, USA) at 488 nm excitation wavelength and using a 585 and 530 nm emission band-pass filter. A minimum of 30000 events per sample was analyzed. Data processing was performed using FlowJo software version 10.5.0 for Windows (FlowJo LCC, Ashland, OR, USA).

Western blot

Whole cell lysates were collected directly after 6 h and 24 h for Western blot analyses. Therefore, cells were rinsed with ice cold PBS and collected in lysis buffer, made from RIPA buffer (150 mM NaCl, 50mM TrisHCl, 1% Nonidet P40, 0.25% sodium deoxycholate and 0.1% SDS), supplemented with 1 mM phenylmethylsulfonyl fluoride, 2 mM Na₃VO₄, 1 mM dithiothreitol, 1 mM sodium pyrophosphate and protease inhibitor mixture (17 μ M leupeptin, 1 μ M aprotinin and 12 μ M pepstatin (all three from Sigma Aldrich)). After centrifugation at 14000 g, 4 °C for 10 min, the supernatant was collected and stored at -80 °C until use. Samples were sonicated on ice in repeated short cycles (5 sec, energy mode, 20 Joules, 70% amplitude, repeated for 4 times) using the Low Power ultrasonic systems 2000 Lpt/LPe with microtip (Branson, Danbury, CT, USA).

Western Blotting was performed as described before [22]. Protein levels, determined by the Lowry method, were adjusted to the same concentration for each blot. After overnight incubation with primary antibodies against caveolin 1 (Cav-1, Becton Dickinson, Franklin Lakes, NJ, USA, #610406, 1:20000),

eNOS_{Thr495} (Cell Signaling Technology (CST), Danvers, USA, #9574, 1:200), eNOS_{Ser1177} (CST, #9571, 1:500), eNOS (CST, #9572, 1:1000), GAPDH (Abcam, Cambridge, United Kingdom, #9484, 1:5000), and SGLT2 (Santa Cruz Biotechnology, #sc-393350, 1:500), membranes were washed with PBS containing 0.1% Tween-20 (Sigma) and incubated with the complementary secondary antibody (IRDye, Licor, Lincoln, USA, 1:5000) for 1h at room temperature before they were washed again. The membranes were scanned with the Odyssey CLx operator (Li-Cor) at auto-scan setting for dynamic range, 169 μ m resolution and medium quality and quantification of the bands was performed with Image Studio™ Software (Version 5.2, Li-Cor). For quantification of the band signals, the signal from each band on an immunoblot was normalized to the signal from the most intensive band on the same membrane according to the manufacturer's instructions. Each signal was then normalized to the housekeeping protein GAPDH.

Co-Immunoprecipitation

Whole cell lysates of HCAECs and HUVECs were collected after 6 hours of TNF α or TNF α +EMPA treatment for Co-immunoprecipitation analyses. Samples were lysed and prepared according to the procedure described above (see western blot). All samples were adjusted to 320 μ g and pre cleared with Protein A magnetic beads (CST, Danvers, USA). Protein A magnetic beads were separated from sample using a magnetic separation rack (CST, Danvers, USA). Samples were incubated with the primary antibody Caveolin-1 (Abcam, Cambridge, United Kingdom, ab2910) with rotation overnight at 4 °C. To extract the immunoprecipitated complex samples were incubated with Protein A magnetic beads, under rotation and the immunoprecipitated complexes were extracted with the magnetic rack.

The immunoprecipitated complexes were loaded on SDS page gels and western blotting was carried out as stated above. The following primary antibodies were used: Caveolin-1 (Abcam, Cambridge, United Kingdom, ab2910) and eNOS (CST, Danvers, USA, #9572).

Endothelial cell permeability assay

Cell permeability was assessed 24h after treatment with TNF α with or without EMPA by measuring FITC-labeled BSA concentration across a cell monolayer seeded on a polyester membrane, as described previously [20]. Briefly, confluent cells grown on 12-well plate transwell inserts (filter area 1.12 cm², pore diameter size 0.4 μ m, Corning Costar, Cambridge, MA, USA) were subjected to the treatment protocols, after which FITC-BSA (10 mg/ml) was added to the upper compartment. After 2h incubation at 37°C, samples from the lower compartment were collected to measure for the albumin leakage across the cell monolayer and membrane. Fluorescence was determined by Spectramax M2e plate reader (Molecular devices LLC, St. José, USA) with the software SoftMaxPro 6.5.1. using excitation wavelength at 485 nm with emission at 535 nm.

Cell staining

To study the cellular distribution of vascular endothelial (VE)-cadherin and F-actin, cells were seeded on to gelatin-coated coverslips (VWR, Radnor, PA, USA). After 24h of treatment with vehicle, TNF α or TNF α +EMPA, the monolayer was fixed with 3.7% paraformaldehyde. Cells were rinsed with PBS before permeabilization with 0.01% Triton X-100 (Sigma) and blocking with 1% BSA (PAA Cell Culture Company, Cambridge, UK). F-actin was stained for 30 min with Phalloidin-Rhodamine (Invitrogen, Carlsbad, USA, 1:40). Fixed cells were treated overnight with anti-VE-Cadherin (CST, 1:100) and second antibody goat anti-rabbit DyeLight 488 the next day (Abcam, Cambridge, UK, 1:1500). After a final wash, cover slips were treated with gold anti-Fade reagent (Invitrogen, Carlsbad, USA), which included DAPI for nuclei staining. The cover slips were stored at 4°C and protected from light. Images were taken with a wide-field microscope Leica DM6 B (Wetzlar, Germany) at 40x magnification.

Cell adhesion molecules expression

After 4h of treatment, surface expression of adhesion molecules was assessed by flow cytometry as described previously [19]. One million HUVECs or 500.000 HCAECs were stained with PE-conjugated antibodies (1:32) for ICAM-1 and VCAM-1 (both from Becton Dickinson). Unstained cells (blanco) and cells stained with isotype-matched antibody (Becton Dickinson) were used as controls to assess auto-fluorescence and non-specific staining. Samples were kept on ice until flow cytometry analysis. Data processing was performed using FlowJo software version 10.5.0 for Windows.

Transfection with siRNA for SGLT2

Cells were transfected at a confluence of 50–80% with siRNA for SGLT2 (ID s12955, Thermo Fisher) or negative control siRNA (Silencer Negative control siRNA, Ambion by Thermo Fisher) together with Lipofectamine RNAiMax (Invitrogen by Thermo Fisher) as described previously [20]. After 72 hours, cells were lysed to determine protein knock down using Western blot analysis as described above.

RNA isolation and cDNA synthesis

Total RNA was extracted using the NucleoSpin®RNA Plus kit (Machery-Nagel, The Netherlands) as described by the manufacturer. The concentration and purity of the RNA were determined using the Nanodrop 2000 (Thermo Fisher, The Netherlands).

Total RNA (1 μ g) was converted to complementary DNA (cDNA) with Transcriptor First Strand cDNA Synthesis kit (Roche, The Netherlands). The concentration was determined by Qubit ssDNA assay kit (Thermo Fisher, The Netherlands).

Taqman quantitativePCR (qPCR)

Taqman qPCR was performed using the LightCycler® 480 instrument (Roche, The Netherlands). For this reaction 90 ng cDNA was used for the Taqman® Gene Expression Assays (Applied Biosystems, The Netherlands) ACTB (Beta Actin, Hs99999903_m1), and SLC5A2 (SGLT2, Hs0089462_m1).

Raw data were exported and subsequently converted into the program LC480Converter. The converted data were imported to the LinRegPCR program and baseline correction was carried out [23].

Statistical analysis

All values are presented as the mean \pm SD. The number of experiments is mentioned as 'n', which for the HCAECs stands for each independent experiment from different batches of cell cultures derived from one single donor and for the HUVECs stands for each independent experiment from a different single donor. For each experimental condition, two-six wells with cells were pooled to avoid bias by single well use. Power analysis was conducted with a probability of 0.05 and a power of 0.8. The number of experiments needed was powered to observe an effect of EMPA in TNF α -stimulated cells. We expected at least a change of 25 \pm 10% to be a relevant effect of EMPA on NO, ROS, permeability, eNOS phosphorylation and adhesion molecule expression, thus we needed to study at least n=4 experiments/condition. The statistical analysis was performed using IBM SPSS Statistics 25. Normality distribution of data were tested with the Shapiro-Wilk test. Student t-test was used for comparisons between control and SGLT α -only treated conditions. Comparisons between more than two groups were performed by one-way ANOVA followed by a Dunnett's post hoc test if data were normally distributed. Not normal data were analyzed with Kruskal-Wallis and Mann-Whitney U tests with Bonferroni correction. P-values are shown in each figure and the post hoc tests are indicated as asterisk symbols (*) to show significant differences as compared to the TNF α condition; *** p < 0.001; ** p < 0.01; * p < 0.05.

Results

EMPA and DAPA reduce ROS levels in TNF α -treated HCAECs

We analyzed the effect of EMPA and DAPA treatment on TNF α -induced intracellular ROS generation in HCAECs using live cell imaging. A significant increase in ROS by TNF α (p<0.01 and p<0.001, respectively Fig. 2a and b) and a strong inhibition in the presence of EMPA and DAPA were observed (Fig. 2a, b p<0.05 and p<0.01 respectively).

EMPA and DAPA restore TNF α -induced loss of NO bioavailability in HCAECs

Endothelial NO bioavailability is an important functional component that is essential for cell signaling with neighboring cell types, including cardiomyocytes. Live cell imaging of intracellular NO showed that HCAECs exhibited attenuated NO levels in the presence of TNF α (Fig. 3a). Interestingly, treatment with EMPA (Fig. 3a) and DAPA (Fig. 3b) preserved the NO concentration in TNF α -stimulated HCAECs (Fig. 3a, b).

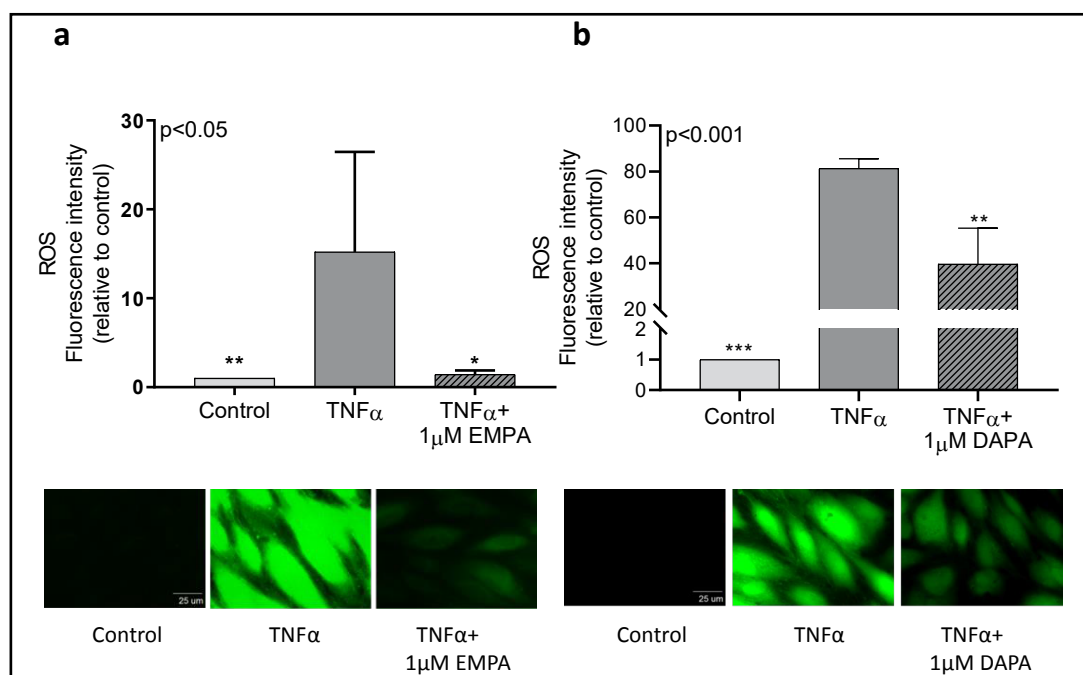


Fig. 2. ROS levels of endothelial cells treated with TNF α , TNF α and EMPA or DAPA. HCAECs were treated with 0.02% DMSO (control), 10 ng/mL TNF α or with 10 ng/mL TNF α with 1 μ M EMPA or DAPA for 6h. ROS levels were measured using live cell imaging in HCAECs (a, n=5, b=n=3) Representative images are shown in the lower panels. Data are presented as mean \pm SD. *p<0.05 vs. TNF α , **p<0.01 vs TNF α .

ROS levels in EMPA treated cells were also investigated using a commercially available FACS assay kit. While ROS generation after 4 h of TNF α stimulation was indeed increased (Supplementary Fig. 2a (HCAECs) and b (HUVECs)), ROS remained unaffected by treatment with 1 μ M EMPA (in mean fluorescence intensity (MFI); HCAECs control 29469 \pm 5411 p<0.05 vs. TNF α , TNF α 47352 \pm 7893, TNF α +EMPA 47433 \pm 8735). To assess whether restoration of ROS levels is detectable using the FACS assay, the anti-oxidant agents N-acetyl cysteine (NAC, 5mM) was administered to HUVECs in additional experiments. These data showed that NAC was able to reverse TNF α -induced ROS formation induced by ROS-inducer Pyocyanin or by TNF α (Supplementary Fig. 3a and b). Moreover, inhibition of ROS by EMPA was not observed in TNF α -stimulated HUVECs using the FACS-based technique (Supplementary Fig. 2b). Furthermore, administration of 1 μ M EMPA alone did not affect ROS levels (Supplementary Fig. 4a and b).

Although live cell imaging in a limited group of experiments with HUVEC revealed for both measurements (ROS and NO) no significant changes between the groups, numerical trends similar as described in HCAECs were observed (Supplementary Fig. 5a, b).

TNF α -induced changes in Cav-1, eNOS signaling and Cav-1/eNOS correlation are not altered by EMPA

NO bioavailability can be modulated by activity and expression of eNOS, which has been previously shown to be altered by TNF α [3, 4,6]. Activity of eNOS is regulated by its subcellular localization and posttranslational modifications. Compartmentalization of the eNOS in caveolae occurs through interaction with Cav-1 and, as previously shown, has an inhibitory effect on eNOS [24]. However, no upregulation of Cav-1 expression was observed in HCAECs after 6 h TNF α stimulation (Fig. 4a+c, arbitrary units, control 0.51 \pm 0.18, TNF α 0.62 \pm 0.19, TNF α +EMPA 0.74 \pm 0.26). HUVECs exposed to TNF α did show increased Cav-1 protein expression after 6 h of incubation compared to control. Nonetheless, treatment with EMPA did not prevent TNF α induced upregulation of Cav-1 in HUVECs (Fig. 4b+c, arbitrary units, control 0.29 \pm 0.10 p<0.001 vs. TNF α , TNF α 0.88 \pm 0.22, TNF α +EMPA 0.89 \pm 0.18).

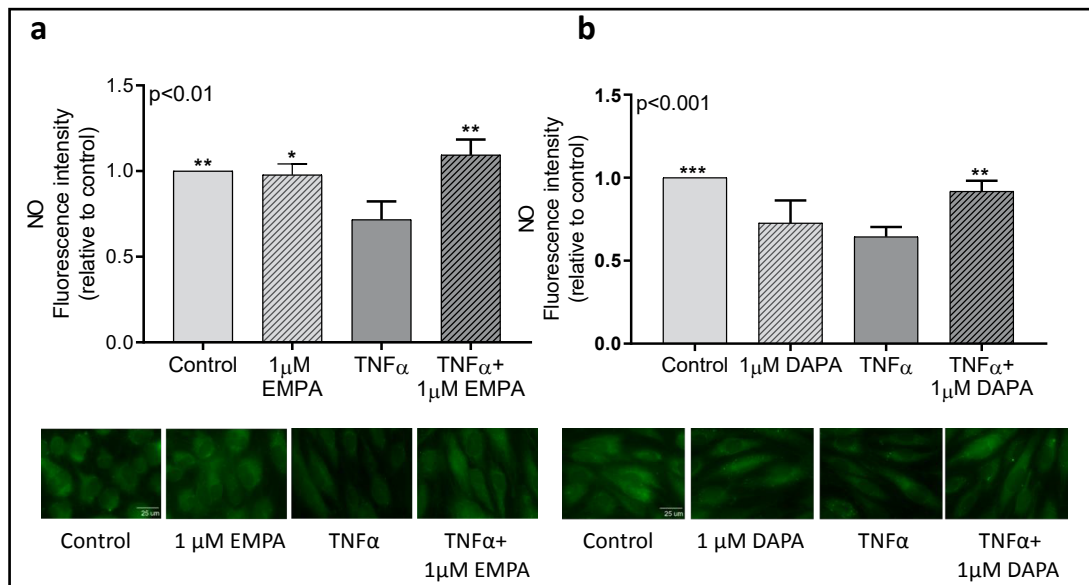


Fig. 3. NO levels of HCAECs treated with TNF α , TNF α and EMPA or DAPA. Cells were treated with 0.02% DMSO (control), 1 μ M EMPA or DAPA, 10 ng/mL TNF α or 10 ng/mL TNF α with 1 μ M EMPA or DAPA for 6h. NO levels were measured using live cell imaging in HCAECs (a,b n=4) Representative images are shown in the panels below each figure. Data are presented as mean \pm SD. *p<0.05 vs. TNF α , **p<0.01, ***p<0.001 vs TNF α .

We performed co-immunoprecipitation with Cav-1 enriched samples from cells subjected to vehicle, TNF α or TNF α +EMPA for 6h after a 2h pre-incubation with vehicle or EMPA. We observed no changes in the interaction between eNOS and caveolin-1 in all three groups in HCAECs and HUVECS, suggesting that the change in caveolin-1 expression after t=6h TNF α is not accompanied with changes in the interaction between eNOS and caveolin-1 (Fig. 4d+e, f).

At 6h TNF α treatment, no significant changes in eNOS_{Ser1177} phosphorylation, total eNOS and eNOS_{Ser1177} expression in HCAECs and HUVECS between the TNF α and the TNF α +EMPA group were found (Fig. 5a-g). Although TNF α induced a slight increase in eNOS_{Ser1177} phosphorylation in HCAECs, EMPA could not prevent this effect (Fig. 5c).

However, when these cells were evaluated after 24h exposure to TNF α , the total amount of eNOS expression was significantly reduced both in HCAECs (Fig. 6b, g) and in HUVECS (Fig. 6e, g). In accordance with the breakdown of total eNOS we found lower levels of phosphorylated eNOS_{Ser1177} as shown by reduced eNOS_{Ser1177}/GAPDH ratio (Fig. 6a+d, g) at 24h. Addition of EMPA had no effect on TNF α downregulated expression of eNOS and its phosphorylated form eNOS_{Ser1177}. Phosphorylation of eNOS was determined by the eNOS_{Ser1177}/eNOS ratio, which did not show any difference between the groups in HUVEC (Fig. 6f, g) and a slight increase of eNOS_{Ser1177} phosphorylation after stimulation with TNF α in HCAECs, which however was not prevented by EMPA treatment (Fig. 6c, g).

These data suggest an increased eNOS reduction or reduced eNOS protein synthesis after 24h TNF α rather than an effect on phosphorylation by TNF α , which in both cases were not be prevented by EMPA.

Similar as in EMPA treated cells, administration of 1 μ M DAPA did not recover eNOS expression or eNOS_{Ser1177} expression (Supplementary Fig. 6) in HCAECs (Supplementary Fig. 6a+e) and HUVECS (Supplementary Fig. 6b+e). However, in the experiments with HCAECs, the eNOS_{Ser1177} expression was not significantly attenuated by TNF α (arbitrary units, Supplementary Fig. 6a HCAECs control 0.78 \pm 0.41, TNF α 0.43 \pm 0.27, TNF α +DAPA 0.63 \pm 0.28; Supplementary Fig. 6b, g HUVECS control 0.99 \pm 0.19 p<0.001 vs. TNF α , TNF α 0.44 \pm 0.15, TNF α +DAPA 0.42 \pm 0.08). eNOS expression was not restored by DAPA in both cell

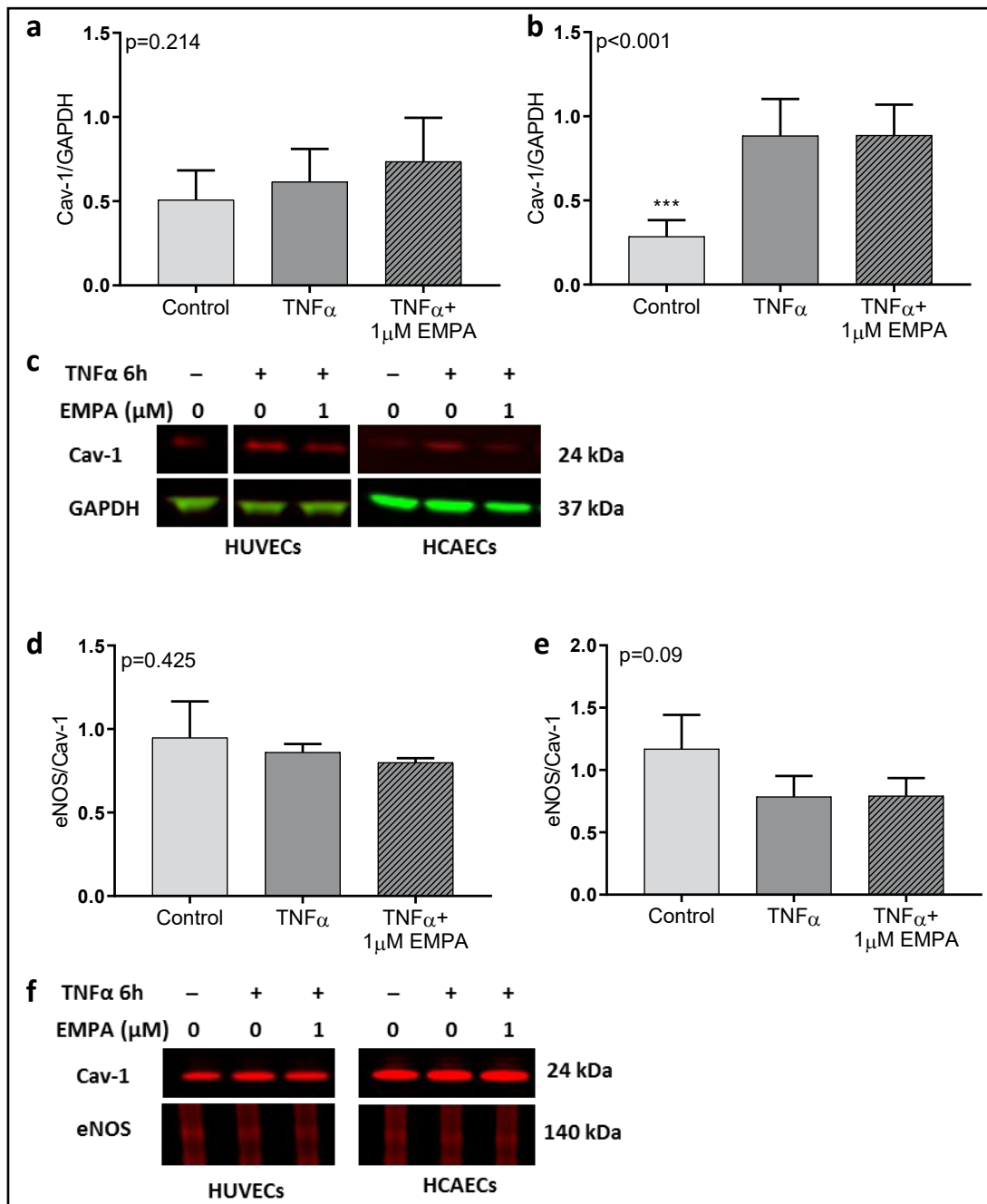


Fig. 4. Protein expression of Cav-1 and co-immunoprecipitation of eNOS/Cav-1 in endothelial cells treated with TNF α and EMPA. Cells were treated with 0.02% DMSO (control), 10 ng/mL TNF α or 10 ng/mL TNF α with 1 μ M EMPA. Cav-1 (Cav-1) levels were determined after 6 h TNF α stimulation in HCAECs (a, n=6) and HUVECs (b, n=6). Representative images of Cav-1 western blots (c). GAPDH was used as internal control. Co-immunoprecipitation of eNOS and Cav-1 in HCAECs (d, n=3) and HUVECs (e, n=3). Representative images of co-immunoprecipitation are shown for HCAECs and HUVECs (f). Unrelated bands omitted for clarity. All full length blots can be found in the supplemental material. Data are presented as mean \pm SD. ** $p<0.01$, *** $p<0.001$ vs. TNF α .

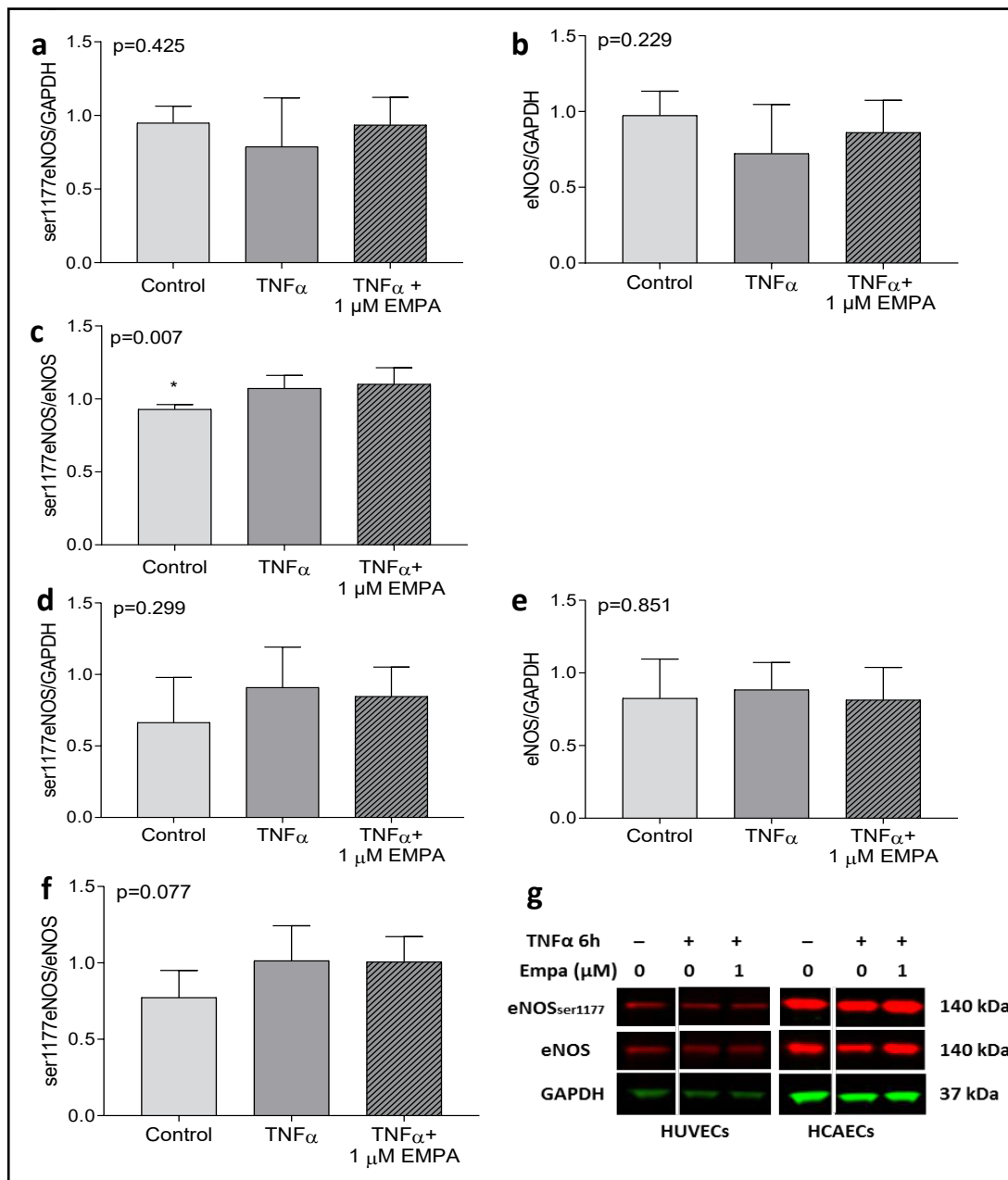


Fig. 5. Protein expression of eNOS_{Ser1177} and total eNOS in endothelial cells treated with TNF α and EMPA after 6 hours. Cells were treated with 0.02% DMSO (control), 10 ng/mL TNF α or 10 ng/mL TNF α with 1 μ M EMPA. eNOS_{Ser1177} and total eNOS levels were determined after 6h TNF α stimulation in HCAECs (a+b, g, n=6) and HUVECs (d+e, g n=6). eNOS_{Ser1177} phosphorylation was determined by the ratio of eNOS_{Ser1177}/eNOS (c,f). Representative images of Western blots for eNOS_{Ser1177} (g) together with total eNOS and GAPDH. Unrelated bands omitted for clarity. All full length blots can be found in the supplemental material. Data are presented as mean \pm SD. * p <0.05 vs. TNF α

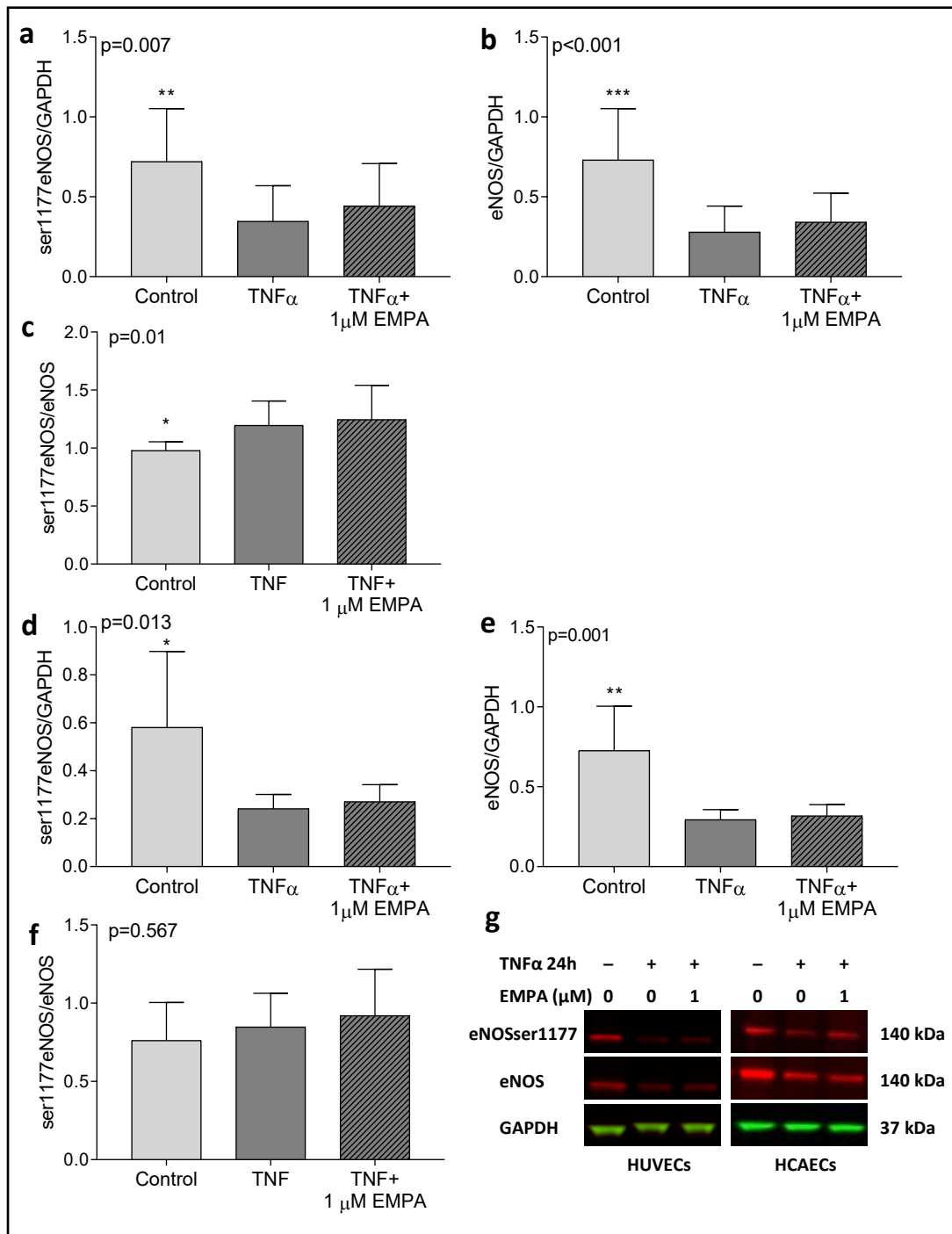


Fig. 6. Protein expression of eNOS_{Ser1177} and total eNOS in endothelial cells treated with TNF α and EMPA after 24 hours. Cells were treated with 0.02% DMSO (control), 10 ng/mL TNF α or 10 ng/mL TNF α with 1 μ M EMPA. eNOS_{Ser1177} and total eNOS levels were determined after 24h TNF α stimulation in HCAECs (a+b, g, n=12) and HUVECs (d+e, g n=6). eNOS_{Ser1177} phosphorylation was determined by the ratio of eNOS_{Ser1177}/eNOS (c,f). Representative images of Western blots for eNOS_{Ser1177} (g) together with total eNOS and GAPDH. All full length blots can be found in the supplemental material. Data are presented as mean \pm SD. **p<0.01, ***p<0.001 vs. TNF α .

types (arbitrary units, Supplementary Fig. 6c HCAECs control 0.89 ± 0.35 $p<0.001$ vs. TNF α , TNF α 0.28 ± 0.08 , TNF α +DAPA 0.33 ± 0.25 ; Supplementary Fig. 6d HUVECs control 1.04 ± 0.21 $p<0.01$ vs. TNF α , TNF α 0.41 ± 0.13 , TNF α +DAPA 0.44 ± 0.05).

In our study the detection of eNOS Thr₄₉₅ showed very high variances between the samples and was technically very challenging (Supplementary Fig. 7a-c). We did not find any difference between the TNF α or TNF α +EMPA treated cells at 6h.

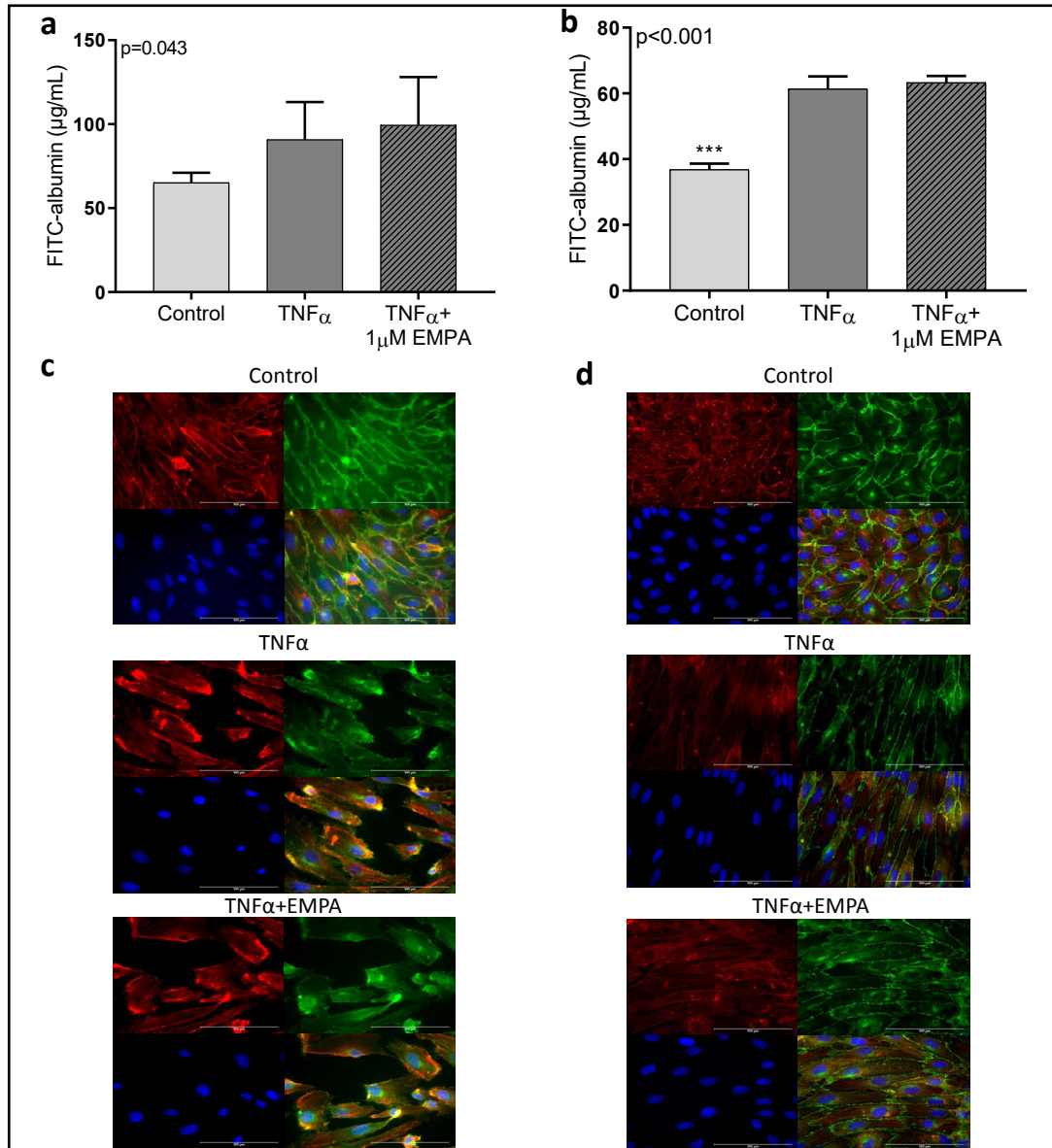


Fig. 7. Endothelial permeability after treatment with TNF α and EMPA. Cells were treated with 0.02% DMSO (control), 10 ng/mL TNF α or with 10 ng/mL TNF α with 1 μ M EMPA. Permeability was subsequently assessed in a trans-well system by assay of 2h FITC-labelled albumin passage through the HCAECs monolayer (a, n=10 trans-wells/condition from three different cell batches) and the HUVECs monolayer (b, n=4 trans-wells/condition). HCAECs (c) and HUVECs (d) seeded on gelatin-coated coverslips were stained for VE-cadherin (green), actin (red) and DAPI (blue) and subjected to treatment as mentioned above. Scale bars represent 100 μ m. Data are presented as mean \pm SD. *** $p<0.001$ vs. TNF α .

No effect of EMPA on TNF α -induced permeability

Elevated permeability was identified after 24h of TNF α stimulation. In HCAECs, TNF α -induced permeability was numerically enhanced with a non-significant trend; administration of EMPA did not affect the permeability in TNF α stimulated HCAECs (Fig. 7a, control 65.2 \pm 5.9, TNF α 90.8 \pm 22.4, TNF α +EMPA 99.4 \pm 28.7). Consistently, administration of EMPA to TNF α -stimulated HUVECs did not attenuate TNF α -induced permeability (in μ g/mL albumin leakage, control 36.8 \pm 1.8 p<0.001 vs. TNF α , TNF α 61.3 \pm 3.8, TNF α +EMPA 63.3 \pm 2.0, Fig. 7b). Fluorescent staining of the cells suggest that HCAECs are slightly more elongated under control condition compared to HUVECs and that TNF α stimulation lead to

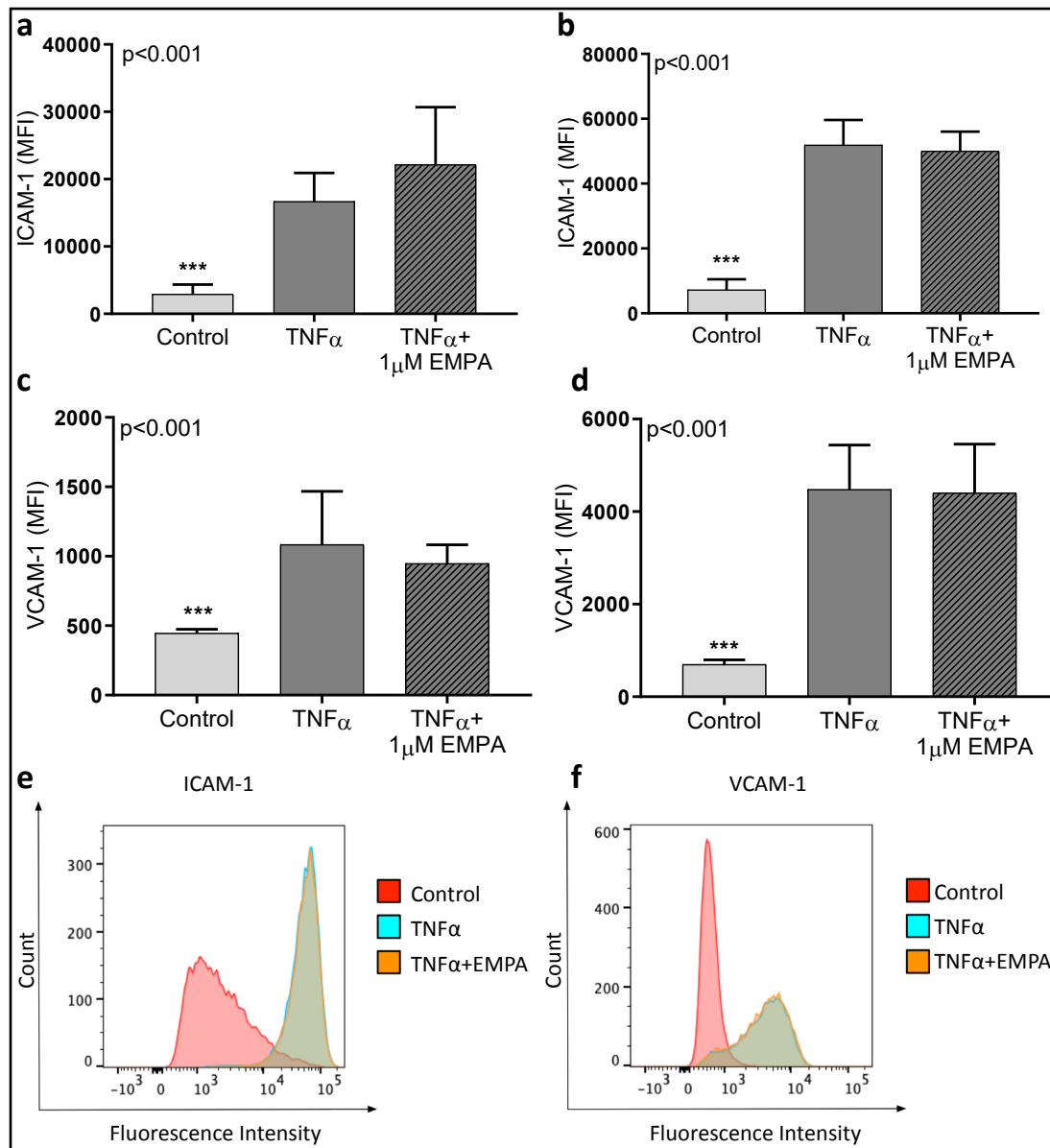


Fig. 8. Expression of adhesion molecules in endothelial cells treated with TNF α and EMPA. Cells were treated with 0.02% DMSO (control), 10 ng/mL TNF α or 10 ng/mL TNF α with 1 μ M EMPA. ICAM-1 levels were determined after 4h TNF α stimulation in HCAECs (a, n=7-8) and HUVECs (b, n=5). VCAM-1 levels were determined after 4h TNF α stimulation in HCAECs (c, n=8) and HUVECs (d, n=5). Representative FACS measurements of ICAM-1 and VCAM-1 for all three conditions (e). Data are presented as mean \pm SD. **p<0.01, ***p<0.001 vs. TNF α .

more pronounced cell-cell gaps in HCAECs vs. HUVECs (Fig. 7c-d). No effect of EMPA-only treatment was observed in both cell types (Supplementary Fig. 8).

TNF α -induced increase in adhesion molecule expression is not attenuated by SGLT2i

Flow cytometry analysis was employed to evaluate the effect of TNF α and EMPA (Fig. 8) on expression of adhesion molecules ICAM-1 and VCAM-1. Measurements of non-labelled and isotope-labelled cells did not differ from the control condition in all experiments (data not shown). TNF α induced a significant upregulation of both adhesion molecules after 4h compared to unstimulated HCAECs (Fig. 8a+c) and HUVECs (Fig. 8b+d). In both cell lines, no significant effect of EMPA was identified on TNF α -induced ICAM-1 (in MFI, HCAECs control 2905 \pm 1448 p <0.001 vs. TNF α , TNF α 16696 \pm 4223, TNF α +EMPA 22139 \pm 8547; HUVECs control 7256 \pm 3237 p <0.001 vs. TNF α , TNF α 51933 \pm 7696, TNF α +EMPA 50004 \pm 6051) and VCAM-1 (in MFI, HCAECs control 446 \pm 28 p <0.001 vs. TNF α , TNF α 1084 \pm 384, TNF α +EMPA 948 \pm 135; HUVECs control 697 \pm 99 p <0.001 vs. TNF α , TNF α 4479 \pm 958, TNF α +EMPA 4403 \pm 1054) expression. A higher dose of EMPA (3 μ M) was investigated, which showed no attenuation of ICAM-1 and VCAM-1 levels in TNF α -stimulated HUVECs (Supplementary Fig. 9a+b).

According to the previous study of Gaspari et al. showing beneficial effects of DAPA on VCAM-1 and ICAM levels in TNF α -stimulated HUVECs after 24h [15], we examined the effects of DAPA in our cells at 24h (Supplementary Fig. 9c-h). Similar to our results with EMPA, addition of 1 μ M DAPA did not attenuate TNF α induced upregulation of ICAM-1 (in MFI, HCAECs, Supplementary Fig. 9c, control 1450 \pm 201 p <0.01 vs. TNF α , TNF α 19308 \pm 4036, TNF α +DAPA 24135 \pm 6706; HUVECs, Supplementary Fig. 9d, control 5814 \pm 1412 p <0.001 vs. TNF α , TNF α 32338 \pm 7308, TNF α +DAPA 34806 \pm 8906) and VCAM-1 (in MFI, HCAECs, Supplementary Fig. 9e, control 450 \pm 9 p <0.001 vs. TNF α , TNF α 1096 \pm 101, TNF α +DAPA 1096 \pm 76; HUVECs, Supplementary Fig. 9f, control 740 \pm 154 p <0.01 vs. TNF α , TNF α 4266 \pm 1791, TNF α +DAPA 3880 \pm 1390).

Involvement of SGLT2 in the observed effects

Western blotting analysis was assessed in order to investigate whether SGLT2 expression is affected by TNF α and whether this may be modulated by EMPA treatment in HUVECs and HCAECs (Supplementary Fig. 10). After 6h incubation, expression of SGLT2 did not change by TNF α in both cell types (Supplementary Fig. 10a+b+e, arbitrary units, HCAECs control 0.70 \pm 0.39, TNF α 0.97 \pm 0.22, TNF α +EMPA 1.00 \pm 0.69; HUVECs control 0.75 \pm 0.37, TNF α 0.74 \pm 0.26, TNF α +EMPA 0.94 \pm 0.17). However, after 24h HUVECs subjected to TNF α showed increased SGLT2 levels as detected by the commercially obtained SGLT2 antibody with no significant difference between TNF α and TNF α +EMPA (Supplementary Fig. 10d+e, arbitrary units, control 0.57 \pm 0.15 p <0.01 vs. TNF α , TNF α 0.90 \pm 0.10, TNF α +EMPA 0.88 \pm 0.11), while SGLT2 expression in HCAECs was not affected by TNF α or TNF α with EMPA (Supplementary Fig. 10c+e, arbitrary units, control 0.50 \pm 0.23, TNF α 0.47 \pm 0.17, TNF α +EMPA 0.48 \pm 0.31).

In order to investigate whether the observed effects of EMPA and DAPA were in fact mediated by SGLT2 inhibition we performed siRNA silencing experiments for SGLT2 in both cell types. Interestingly we were not able to silence SGLT2 protein as detected with the same commercially available antibody in the western blot (Supplementary Fig. 10f). This fact raised the question whether we could detect mRNA of SGLT2 in HCAECs. By qPCR we show that SGLT2 mRNA is in fact not detectable in HCAECs (Supplementary Fig. 10g). Together with the fact that the study of Mancini al. showed that HUVECs also do not express relevant amounts of SGLT2 [17], we therefore cannot exclude that the bands seen in western blot with the commercially available antibody might not be SGLT2 protein.

This suggests that SGLT2 inhibition is probably not involved in the observed anti-inflammatory effects of EMPA and DAPA.

Discussion

In the present study, we investigated whether SGLT2i's exert pleiotropic effects on arterial and venous endothelial cells stimulated with TNF α . Our data showed that EMPA and DAPA reduce ROS levels and restore NO bioavailability in TNF α -stimulated HCAECs. TNF α -induced changes of endothelial monolayer permeability were unresponsive to EMPA treatment. EMPA and DAPA neither prevent the increased adhesion molecules expression after TNF α stimulation nor eNOS phosphorylation or expression. Taken together, these data suggest that SGLT2i's EMPA and DAPA directly intervene with TNF α -induced endothelial dysfunction by reducing ROS levels and restoring NO bioavailability.

EMPA and DAPA restore NO bioavailability after TNF α stimulation without affecting eNOS phosphorylation or expression

Changes in intracellular NO concentrations were determined after 6h treatment with TNF in the presence or absence of EMPA and DAPA. We observed a restoration in NO bioavailability by EMPA and DAPA in TNF α -stimulated HCAECs. TNF α can modulate NO bioavailability by directly affecting the phosphorylation or expression of eNOS [3, 4,6] and by increasing the intracellular superoxide levels [6, 25]. At 6h after treatment with TNF α we did not find significant changes between the TNF α and the TNF α +EMPA group in both cell types suggesting that phosphorylation of eNOS Ser1177 and eNOS signaling is not involved in the strong reduction of ROS by EMPA and DAPA at that time.

We observed 50-60% reduction in eNOS_{Ser1177} and total eNOS expression in 24h TNF α stimulated HUVECs and HCAECs. Since not only phosphorylated eNOS, but also total expression, was reduced by TNF α , it is most likely that TNF α under these conditions resulted in decreased synthesis or elevated breakdown of eNOS (mRNA) rather than acting on phosphorylation of eNOS [3, 6]. We did, however, not observe a restoration of eNOS phosphorylation and eNOS expression by EMPA or DAPA. Conversely, TNF α -induced ROS generation was completely abolished by both SGLT2i's in HCAECs, which may suggest that EMPA and DAPA affect NO bioavailability by inhibiting the generation of ROS (further discussed in the next section).

There are several studies showing vasodilation effects of SGLT2i's. In *ex vivo* intact mouse hearts, we observed acute vasodilation by 1 μ M EMPA treatment [26]. The direct effect of EMPA observed in that study may be associated with inhibition of the sodium/hydrogen exchanger 1 (NHE-1) in cardiomyocytes [26–29]. Although inhibition of endothelial NHE-1 has also been linked to improved endothelial cell function [30, 31], it remains unknown whether NHE-1 was actually inhibited in the TNF α -stimulated HUVECs and HCAECs in the present study. Furthermore, EMPA was shown to preserve vasodilator response and eNOS expression in vascular rings [32] and recovered nitrite levels in cultured HUVECs during hyperglycemia [33]. Effects of EMPA on vascular rings were suggested to be linked to SGLT2 inhibition in endothelial cells [33]. However, using vascular rings, effects on vascular smooth muscle cell function cannot be excluded.

The role of Cav-1 in endothelial cells has previously been associated within TNF α -induced signaling. Cav-1 downregulation resulted in improved monolayer integrity in rat pulmonary microvascular endothelial cells stimulated with TNF α [34]. Moreover, elevated Cav-1 levels have been observed in endothelial cells subjected to TNF α [35]. In contrast, our data show no TNF α -induced Cav-1 upregulation in HCAECs. Knowing that Cav-1 plays a major role in endothelial signaling pathways in vascular pathologies, further studies should explore to what extent Cav-1 signaling is divergent in HCAECs compared to other endothelial cells.

Interestingly, co-immunoprecipitation of eNOS and Cav-1 in both cell types revealed no significant changes in the co-immunoprecipitated complexes between TNF α and TNF α +EMPA treated cells. These data further strengthen the hypothesis that EMPA does not modulate localization of eNOS in proximity to Cav-1.

Regarding the second (inhibitory) phosphorylation site of eNOS, eNOS_{Thr495}, the recent study of Steven et al. showed that EMPA treatment inhibits this phosphorylation site [32]. The authors suggest that the improved NO/cGMP signaling they measured is not based on upregulation of eNOS gene expression but rather on prevention of oxidative damage of the NO/cGMP signaling pathway [32].

Since this study was also performed in animals, it cannot be excluded that the effects of EMPA on peNOS_{Thr495} are not specifically a direct effect on endothelial cells.

Combined, the results of the present study propose that EMPA and DAPA restore NO bioavailability rather by a pathway not involving eNOS phosphorylation, expression or signaling.

EMPA and DAPA attenuate TNF α -induced increase in ROS

An elevation in ROS levels is an important hallmark of endothelial dysfunction [36]. Using live cell imaging, we observed that TNF α significantly elevated ROS levels and that treatment with EMPA or DAPA completely inhibited the TNF α -induced upregulation of intracellular ROS levels. Our data correspond to a previous report showing total inhibition of ROS by EMPA in TNF α -stimulated cardiac microvascular endothelial cells [18]. These effects could not be explained by a direct ROS scavenging effect of EMPA [18]. To our knowledge for DAPA no report exist that shows this strong inhibition of DAPA on TNF α -induced ROS levels in endothelial cells. Therefore, the inhibition of inflammation-induced oxidative stress by SGLT2i's seems to be a class effect of these novel anti-diabetic drug.

We also investigated intracellular ROS using a FACS-based commercially available technique. ROS levels were expected to be increased in TNF α -stimulated endothelial cells, which was indeed the case with a ~50% increase in ROS after 4 h TNF α stimulation (Supplementary Fig. 3). However, no effect of EMPA on ROS was observed in both HUVECs and HCAECs. An important difference between the FACS-based measurements and the live cell imaging technique is that the latter is able to measure all intracellular ROS, including super-oxide, while super-oxide cannot be detected by the FACS assay. Furthermore, when employing the FACS technique TNF α and/or EMPA were not present at the time the suspended cells were loaded with the ROS probe, thus an acute EMPA effect might not be measured with this technique. In accordance with our data from live cell imaging, it was reported that mitochondrial ROS was inhibited by EMPA in cardiac microvascular endothelial cells stimulated with TNF α [18].

Previous *in vitro* investigations have reported divergent effects of SGLT2i's on intracellular ROS in non-endothelial cell types. Pre-incubation of EMPA in Tacrolimus-induced human kidney 2 (HK-2) cells reduced the burst of intracellular ROS levels at concentrations of 100 and 500 nM [37]. In cultured LPS-induced macrophages, canagliflozin (CANA) reduced oxidative stress and exhibited anti-inflammatory effects after 3-12 hours [38]. The effects were likely due to the inhibition of glucose metabolism and an increase in autophagy. However, reduced ROS was only observed at high dosages (>20 μ M) of CANA. In differentiated renal proximal tubule epithelial cells, super-oxide production was not affected at clinically relevant dosages of EMPA, DAPA and CANA. Conversely ≥ 50 μ M CANA did induce super-oxide production, suggesting a cytotoxic effect of the drug at higher concentrations [39]. Overall, the effects of SGLT2i's on intracellular ROS is concentration-, SGLT2i type- and cell type-dependent. Further studies should unravel under which conditions SGLT2i's reduce ROS and should also investigate which other cellular mechanisms related to ROS are affected by SGLT2i's.

No direct improvement in cell-cell adhesion by SGLT2i's

Direct anti-inflammatory actions of SGLT2i's CANA and DAPA have been observed previously in HUVECs using inflammatory stimuli, including IL-1 β or TNF α [15, 40]. In HUVECs and HCAECs, EMPA did not attenuate the TNF α -induced upregulation of endothelial cell permeability, and expression of VCAM-1 and ICAM-1. These data are in line with previous findings in HUVECs showing no effect of EMPA or DAPA on IL-6 and MCP-1 secretion in IL-

1 β -stimulated HUVECs [17]. Conversely, a previous study reported that low doses of DAPA possess direct anti-atherogenic effects in cultured HUVECs by attenuation of TNF α -induced VCAM-1 and ICAM-1 expression after 24h [15]. Possible divergent results between these studies may lie in the inflammatory stimuli (IL-1 β vs. TNF α) as well as the concentration SGLT2i used (1 μ M vs. 1-5nM respectively), which both differed in those studies. With regard to protective effects of DAPA observed at lower dosages, we also performed pilot studies that included lower doses of DAPA (1 and 10 nM), which showed no changes in adhesion molecules and phosphorylated eNOS expression. Therefore, these concentrations were not further explored by us (data not shown).

The way SGLT2i's could directly affect endothelial cell function under inflammatory conditions is still debated [28]. Increased 5' AMP-activated protein kinase (AMPK) activity through inhibition of mitochondrial complex 1 by CANA has been postulated to be involved in the anti-inflammatory effect of CANA, although this pathway seems to be only affected by CANA and not by DAPA or EMPA [17, 40]. It becomes more apparent that SGLT2i's possess drug-specific effects on intracellular mechanisms and cell function in endothelial cells. Mancini et al. reported that cell adhesion molecules expression and NF κ B signaling were not affected at a clinically relevant concentrations of CANA [17], which supports our data showing no effect of EMPA on TNF α -induced adhesion molecule expression. Overall, data from our study offer evidence that both EMPA and DAPA do not attenuate permeability, VCAM-1 and ICAM-1 expression in TNF α stimulated HCAECs and HUVECs.

Finally, our data from the quantitative measurement of endothelial permeability and the fluorescent staining of the endothelial monolayer suggest that baseline monolayer permeability was higher in HCAECs (Fig. 7a) compared to HUVECs (Fig. 7b). The HCAECs may have possibly been more responsive to the different stimuli compared to the HUVECs. Evidently, the use of these two different endothelial cell types indicates to some extent a divergence character and response for HCAECs and HUVECs as for HUVECs we did not find a significant effect on NO or ROS measured by live cell imaging, though especially ROS measurements clearly showed the same trend as in HCAECs (Supplementary Fig. 5).

Expression of SGLT2 in endothelial cells

The presence of SGLT2 in endothelial cells is currently discussed and several studies have explored SGLT2 expression at the protein and mRNA level in endothelial cells [33, 41, 42]. A very recent study showed elevated mRNA and protein SGLT2 expression levels in porcine coronary artery endothelial cells exposed to H₂O₂ or high glucose [43]. This study did show that 100 nM EMPA reduced SGLT2 protein expression in high glucose porcine coronary artery segments, although no change in the activity of SGLT2 by EMPA was observed.

We have explored SGLT2 protein expression in HUVECs and HCAECs using a commercially available antibody for SGLT2. In both cell types, western blot analysis of SGLT2 suggested that SGLT2 protein is expressed. This was shown by a corresponding band on the immunoblot (Supplementary Fig. 10). Regarding the interpretation of the SGLT2 protein band our data showed increased SGLT2 expression already after 24h of TNF α stimulation, although this effect was only detected in HUVECs and not HCAECs. In both cell types, EMPA did not alter the expression of SGLT2. In contrast, in kidney epithelial cells, TNF α (10 pg/mL) stimulated SGLT2 mRNA only after 4 days and SGLT2 expression after 5 days [44].

However, while we aimed to answer the question whether the observed effects of EMPA are actually mediated via SGLT2 we struggled upon the fact that we were unable to silence the SGLT2 protein expression in both cell types using siRNA for SGLT2. Thus, we performed quantitative PCR to measure mRNA levels for SGLT2 in HCAECs, and could not detect any SGLT2 mRNA. Taken this together with the fact that Mancini and co-workers did not find SGLT2 mRNA in human umbilical vein endothelial cells and human aortic endothelial cells [17] raises the concern that although the antibody used to detect SGLT2 was specific for human SGLT2, the expression of SGLT2 mRNA in endothelial cells is very questionable and will need further investigations.

Study limitations

In all our experiments, the experimental and culture conditions lacked flow, which may have affected endothelial activity as well as the expression of particular membrane receptors. Furthermore, we only studied the effects of the SGLT2 inhibitors on endothelial cells obtained from non-diabetic subjects and at normo-glycemic conditions. Previous studies have reported an increased activity of endothelial cells or endothelial dysfunction with elevated glucose concentrations [30, 45–47]. We have performed extensive experiments at various glucose concentrations, however we did not observe a decline in endothelial function and activity, i.e. eNOS phosphorylation, adhesion molecules expression and ROS levels after 24-72h of hyperglycemia (unpublished data). Further research should investigate the effects of SGLT2 inhibitors in diabetic endothelial cells or at high glucose concentrations in combination with an inflammatory stimulus. Furthermore, the experiments with HCAECs were performed in a commercially available cell line derived from one donor, so a complete generalization of these results is only possible to a limited extent as we cannot know how a different donor would have responded to the treatments.

Although we observed a significant reduction in the total eNOS levels in these experiments, we cannot exclude the fact that the downregulation of eNOS phosphorylation by TNF α was not significant in the DAPA experiments due to low n (n=6-8 in DAPA experiments vs. n=12 in EMPA experiments).

Considering the TNF α dosage used, our pilot data with 2ng/mL showed no significant reduction in eNOS expression, therefore we chose to use 10ng/mL TNF α as a model of endothelial inflammation. This concentration of TNF α has been previously observed in several patients populations [48, 49], therefore it may remain of physiological significance. However, inflammation remains a complex signaling cascade and the use of only TNF α to induce inflammation may have been insufficient to study endothelial inflammatory mechanisms.

Conclusion

Empagliflozin and Dapagliflozin restore NO bioavailability, possibly via the reduction in ROS generation in TNF α -stimulated HCAECs. The anti-inflammatory effects of SGLT2i's Empagliflozin and Dapagliflozin do not appear to be mediated via eNOS phosphorylation/expression and changes in adhesion molecules expression. Our study provides novel insights into the direct cellular effects of SGLT2i's in the endothelium.

Abbreviations

SGLT2 (Sodium glucose co-transporter 2); SGLT2i's (Sodium glucose co-transporter 2 inhibitor(s)); TNF α (Tumor necrosis factor α); HUVECs (Human umbilical vein endothelial cells); HCAECs (Human coronary arterial endothelial cells); VCAM-1 (Vascular cell Adhesion molecule -1); ICAM-1 (Intercellular Adhesion Molecule -1); eNOS (Endothelial nitric oxide synthase); eNOS_{Ser1177} (Endothelial nitric oxide synthase phosphorylated at Serine 1177); T2D (Type 2 diabetes); ROS (Reactive oxygen species); EMPA (Empagliflozin); DAPA (Dapagliflozin); CANA (Canagliflozin); IL-1 β (Interleukin-1 β); FITC (Fluorescein isothiocyanate); VE-cadherin (Vascular endothelial cadherin); Cav-1 (Caveolin - 1); GAPDH (Glyceraldehyde 3-phosphate dehydrogenase); vWF (Von Willebrand Factor); MFI (Mean fluorescence intensity); NAC (N-acetyl cysteine); HK-2 cells (Human kidney 2 cells); LPS (Lipopolysaccharide); IL-6 (Interleukin - 6); MCP-1 (Monocyte Chemoattractant Protein-1); FACS (Fluorescence-activated cell sorting); PC (Pyocyanin); ACTB (Actin beta (gene)).

Acknowledgements

We acknowledge the Cellular Imaging, Core Facility of the Amsterdam UMC location AMC, especially Przemek Krawczyk and Ron Hoebe for their expertise and assistance with establishing the live cell imaging experiments.

Statement of ethics

The isolation of HUVECs from human umbilical cords has been waived by the medical ethical committee: W12-167#12.17.096 Amsterdam, the Netherlands.

Funding sources

R. P. Juni is supported by a grant of the Netherlands Heart Foundation (CVON-RECONNECT). C. J. Z was supported by EFSD/Novo Nordisk.

Author's contribution

MWH, BP, PK, VH, CJZ and MA contributed to the analysis planning and interpretation of data, and reviewed and edited the manuscript. RPJ, ELS, MB and RK contributed to the acquisition of data, analysis and interpretation of data, and reviewed the manuscript. LU, AH and NCW contributed to the conception and design, acquisition of data and analysis and interpretation of data, and drafting and revising the critical intellectual content of the manuscript. All authors were fully responsible for all content and approved the final version. NCW is guarantor of this work.

Disclosure Statement

The authors have no conflicts of interest to declare.

References

- 1 Natali A, Toschi E, Baldeweg S, Ciociaro D, Favilla S: Clustering of Insulin Resistance With Vascular Dysfunction and Low-Grade Inflammation in Type 2 Diabetes. *Diabetes* 2006;55:1133-1140.
- 2 Dewi BE, Takasaki T, Kurane I: *In vitro* assessment of human endothelial cell permeability: Effects of inflammatory cytokines and dengue virus infection. *J Virol Methods* 2004;121:171-180.
- 3 Yan G, You B, Chen SP, Liao JK, Sun J: Tumor necrosis factor- α downregulates endothelial nitric oxide synthase mRNA stability via translation elongation factor 1- α 1. *Circ Res* 2008;103:591-597.
- 4 Kim J, Lee KS, Kim JH, Lee DK, Park M, Choi S, Park W, Kim S, Choi YK, Hwang JY, Choe J, Won MH, Jeoung D, Lee H, Ryoo S, Ha KS, Kwon YG, Kim YM: Aspirin prevents TNF- α -induced endothelial cell dysfunction by regulating the NF- κ B-dependent miR-155/eNOS pathway: Role of a miR-155/eNOS axis in preeclampsia. *Free Radic Biol Med* 2017;104:185-198.
- 5 Pan LL, Liu XH, Gong QH, Wu D, Zhu YZ: Hydrogen sulfide attenuated tumor necrosis factor- α -induced inflammatory signaling and dysfunction in vascular endothelial cells. *PLoS One* 2011;6:e19766.
- 6 Zhang H, Park Y, Wu J, Chen Xp, Lee S, Yang J, Dellsperger KC, Zhang C: Role of TNF- α in vascular dysfunction. *Clin Sci* 2009;116:219-230.
- 7 Zinman B, Wanner C, Lachin JM, Fitchett D, Bluhmki E, Hantel S, Mattheus M, Devins T, Johansen OE, Woerle HJ, Broedl UC, Inzucchi SE; EMPA-REG OUTCOME Investigators: Empagliflozin, Cardiovascular Outcomes, and Mortality in Type 2 Diabetes. *N Engl J Med* 2015;373:2117-2128.
- 8 Neal B, Perkovic V, Mahaffey KW, de Zeeuw D, Fulcher G, Erondou N, Shaw W, Law G, Desai M, Matthews DR, CANVAS Program Collaborative Group: Canagliflozin and Cardiovascular and Renal Events in Type 2 Diabetes. *N Engl J Med* 2017;377:644-657.

- 9 Wiviott SD, Raz I, Bonaca MP, Mosenzon O, Kato ET, Cahn A, Silverman MG, Zelniker TA, Kuder JF, Murphy SA, Bhatt DL, Leiter LA, McGuire DK, Wilding JPH, Ruff CT, Gause-Nilsson IAM, Fredriksson M, Johansson PA, Langkilde AM, Sabatine MS, et al.: Dapagliflozin and Cardiovascular Outcomes in Type 2 Diabetes. *N Engl J Med* 2019;380:347-357.
- 10 Ye Y, Bajaj M, Yang HC, Perez-Polo JR, Birnbaum Y: SGLT-2 Inhibition with Dapagliflozin Reduces the Activation of the Nlrp3/ASC Inflammasome and Attenuates the Development of Diabetic Cardiomyopathy in Mice with Type 2 Diabetes. Further Augmentation of the Effects with Saxagliptin, a DPP4 Inhibitor. *Cardiovasc Drugs Ther* 2017;31:119-132.
- 11 Han JH, Oh TJ, Lee G, Maeng HJ, Lee DH, Kim KM, Choi SH, Jang HC, Lee HS, Park KS, Kim YB, Lim S: The beneficial effects of empagliflozin, an SGLT2 inhibitor, on atherosclerosis in ApoE $-/-$ mice fed a western diet. *Diabetologia* 2017;60:364-376.
- 12 Lin B, Koibuchi N, Hasegawa Y, Sueta D, Toyama K, Uekawa K, Ma M, Nakagawa T, Kusaka H, Kim-Mitsuyama S: Glycemic control with empagliflozin, a novel selective SGLT2 inhibitor, ameliorates cardiovascular injury and cognitive dysfunction in obese and type 2 diabetic mice. *Cardiovasc Diabetol* 2014;13:148.
- 13 Lee TM, Chang NC, Lin SZ: Dapagliflozin, a selective SGLT2 Inhibitor, attenuated cardiac fibrosis by regulating the macrophage polarization via STAT3 signaling in infarcted rat hearts. *Free Radic Biol Med* 2017;104:298-310.
- 14 Zhou H, Wang S, Zhu P, Hu S, Chen Y, Ren J: Empagliflozin rescues diabetic myocardial microvascular injury via AMPK-mediated inhibition of mitochondrial fission. *Redox Biol* 2018;15:335-346.
- 15 Gaspari T, Spizzo I, Liu H, Hu Y, Simpson RW, Widdop RE, Dear AE: Dapagliflozin attenuates human vascular endothelial cell activation and induces vasorelaxation: A potential mechanism for inhibition of atherogenesis. *Diabetes Vasc Dis Res* 2017;15:64-73.
- 16 Andreadou I, Efentakis P, Balafas E, Togliatto G, Davos CH, Varela A, Dimitriou CA, Nikolaou PE, Maratou E, Lambadiari V, Ikonomidis I, Kostomitsopoulos N, Brizzi MF, Dimitriadis G, Iliodromitis EK: Empagliflozin limits myocardial infarction *in vivo* and cell death *in vitro*: Role of STAT3, mitochondria, and redox aspects. *Front Physiol* 2017;8:1077.
- 17 Mancini SJ, Boyd D, Katwan OJ, Strembitska A, Almabrouk TA, Kennedy S, Palmer TM, Salt IP: Canagliflozin inhibits interleukin-1 β -stimulated cytokine and chemokine secretion in vascular endothelial cells by AMP-activated protein kinase-dependent and -independent mechanisms. *Sci Rep* 2018;8:5276.
- 18 Juni RP, Kuster DWD, Goebel M, Helmes M, Velden J Van Der, Koolwijk P, Paulus WJ, van Hinsbergh VWM: Cardiac Microvascular Endothelial Enhancement of Cardiomyocyte Function is Impaired by Inflammation and Restored by Empagliflozin. *JACC Basic Transl Sci* 2019;4:575-591.
- 19 Weber NC, Kandler J, Schlack W, Grueber Y, Fradorf J, Preckel B: Intermittent pharmacologic pretreatment by xenon, isoflurane, nitrous oxide, and the opioid morphine prevents tumor necrosis factor alpha-induced adhesion molecule expression in human umbilical vein endothelial cells. *Anesthesiology* 2008;108:199-207.
- 20 Smit KF, Konkel M, Kerindongo R, Landau MA, Zuurbier CJ, Hollmann MW, Preckel B, Nieuwland R, Albrecht M, Weber NC: Helium alters the cytoskeleton and decreases permeability in endothelial cells cultured *in vitro* through a pathway involving Caveolin-1. *Sci Rep* 2018;8:4768.
- 21 Cossarizza A, Ferraresi R, Troiano L, Roat E, Gibellini L, Bertonecelli L, Nasi M, Pinti M: Simultaneous analysis of reactive oxygen species and reduced glutathione content in living cells by polychromatic flow cytometry. *Nat Protoc* 2009;4:1790-1797.
- 22 Smit KF, Brevoord D, De Hert S, de Mol BA, Kerindongo RP, van Dieren S, Schlack WS, Hollmann MW, Weber NC, Preckel B: Effect of helium pre- or postconditioning on signal transduction kinases in patients undergoing coronary artery bypass graft surgery. *J Transl Med* 2016;14:294.
- 23 Ramakers C, Ruijter JM, Lekanne Deprez RH, Moorman AFM: Assumption-free analysis of quantitative real-time polymerase chain reaction (PCR) data. *Neurosci Lett* 2003;339:62-66.
- 24 Bernatchez PN, Bauer PM, Prendergast JS, Prendergast JS, He P, Sessa WC: Dissecting the molecular control of endothelial NO synthase by caveolin-1 using cell-permeable peptides. *Proc Natl Acad Sci* 2005;102:761-766.
- 25 Zhao Y, Vanhoutte PM, Leung SWS: Vascular nitric oxide: Beyond eNOS. *J Pharmacol Sci* 2015;129:83-94.
- 26 Uthman L, Baartscheer A, Bleijlevens B, Schumacher CA, Fiolet JWT, Koeman A, Jancev M, Hollmann MW, Weber NC, Coronel R, Zuurbier CJ: Class effects of SGLT2 inhibitors in mouse cardiomyocytes and hearts: inhibition of Na $^+$ /H $^+$ exchanger, lowering of cytosolic Na $^+$ and vasodilation. *Diabetologia* 2018;61:722-726.

- 27 Uthman L, Nederlof R, Eerbeek O, Baartscheer A, Schumacher C, Buchholtz N, Hollmann MW, Coronel R, Weber NC, Zuurbier CJ: Delayed ischaemic contracture onset by empagliflozin associates with NHE1 inhibition and is dependent on insulin in isolated mouse hearts. *Cardiovasc Res* 2019;115:1533-1545.
- 28 Uthman L, Baartscheer A, Schumacher CA, Fiolet JWT, Kuschma MC, Hollmann MW, Coronel R, Weber NC, Zuurbier CJ: Direct Cardiac Actions of Sodium Glucose Cotransporter 2 Inhibitors Target Pathogenic Mechanisms Underlying Heart Failure in Diabetic Patients. *Front Physiol* 2018;9:1575.
- 29 Arjun S, Bell RM. SGLT2 inhibitors: reviving the sodium-hydrogen exchanger cardioprotection hypothesis? *Cardiovasc Res* 2019;115:1454-1456.
- 30 Wang S, Peng Q, Zhang J, Liu L: Na⁺/H⁺exchanger is required for hyperglycaemia- induced endothelial dysfunction via calcium-dependent calpain. *Cardiovasc Res* 2008;80:255-262.
- 31 Cui GM, Zhao YX, Zhang NN, Liu ZS, Sun WC, Peng QS: Amiloride attenuates lipopolysaccharide-accelerated atherosclerosis via inhibition of NHE1-dependent endothelial cell apoptosis. *Acta Pharmacol Sin* 2013;34:231-238.
- 32 Steven S, Oelze M, Hanf A, Kröller-Schön S, Kashani F, Roohani S, Welschhof P, Kopp M, Gödtel-Armbrust U, Xia N, Li H, Schulz E, Lackner KJ, Wojnowski L, Bottari SP, Wenzel P, Mayoux E, Münzel T, Daiber A: The SGLT2 inhibitor empagliflozin improves the primary diabetic complications in ZDF rats. *Redox Biol* 2017;13:370-385.
- 33 El-daly M, Krishna V, Venu P, Mihara K, Kang S, Fedak PWM, Alston LA, Hirota SA, Ding H, Triggle CR, Hollenberg MD: Hyperglycaemic impairment of PAR2-mediated vasodilation: Prevention by inhibition of aortic endothelial sodium-glucose-co- Transporter-2 and minimizing oxidative stress. *Vascul Pharmacol* 2018;109:56-71.
- 34 Shao M, Yue Y, Sun GY, You QH, Wang N, Zhang D: Caveolin-1 Regulates Rac1 Activation and Rat Pulmonary Microvascular Endothelial Hyperpermeability Induced by TNF- α . *PLoS One* 2013;8:e55213.
- 35 Wang L, Lim E-J, Toborek M, Hennig B: The role of fatty acid and caveolin1 in TNF-alpha-induced endothelial cell activation. *Metabolism* 2008;57:1328-1339.
- 36 Incalza MA, D'Oria R, Natalicchio A, Perrini S, Laviola L, Giorgino F: Oxidative stress and reactive oxygen species in endothelial dysfunction associated with cardiovascular and metabolic diseases. *Vascul Pharmacol* 2018;100:1-19.
- 37 Jin J, Jin L, Luo K, Lim SW, Chung BH, Yang CW: Effect of Empagliflozin on Tacrolimus-Induced Pancreas Islet Dysfunction and Renal Injury. *Am J Transplant* 2017;17:2601-2616.
- 38 Xu C, Wang W, Zhong J, Lei F, Xu N, Zhang Y, Xie W: Canagliflozin exerts anti-inflammatory effects by inhibiting intracellular glucose metabolism and promoting autophagy in immune cells. *Biochem Pharmacol* 2018;152:45-59.
- 39 Secker PF, Beneke S, Schlichenmaier N, Delp J, Gutbier S, Leist M, Dietrich DR: Canagliflozin mediated dual inhibition of mitochondrial glutamate dehydrogenase and complex I: an off-target adverse effect article. *Cell Death Dis* 2018;9:226.
- 40 Hawley SA, Ford RJ, Smith BK, Gowans GJ, Mancini SJ, Pitt RD, Day EA, Salt IP, Steinberg GR, Hardie DG: The Na⁺/Glucose Cotransporter Inhibitor Canagliflozin Activates AMPK by Inhibiting Mitochondrial Function and Increasing Cellular AMP Levels. *Diabetes* 2016;65:2784-2794.
- 41 Zhou L, Cryan E V, D'Andrea MR, Belkowski S, Conway BR, Demarest KT: Human cardiomyocytes express high level of Na⁺/glucose cotransporter 1 (SGLT1). *J Cell Biochem* 2003;90:339-346.
- 42 Li CY, Wang LX, Dong SS, Hong Y, Zhou XH, Zheng WW, Zheng C: Phlorizin Exerts Direct Protective Effects on Palmitic Acid (PA)-Induced Endothelial Dysfunction by Activating the PI3K/AKT/eNOS Signaling Pathway and Increasing the Levels of Nitric Oxide (NO). *Med Sci Monit Basic Res* 2018;24:1-9.
- 43 Khemais-Benkhiat S, Belcastro E, Idris-Khodja N, Park S, Amoura L, Abbas M, Auger C, Kessler L, Mayoux E, Toti F, Schini-Kerth VB: Angiotensin II-induced redox-sensitive SGLT1 and 2 expression promotes high glucose-induced endothelial cell senescence. *J Cell Mol Med* 2019; DOI:10.1111/jcmm.14233.
- 44 Maldonado-Cervantes MI, Galicia OG, Moreno-Jaime B, Zapata-Morales JR, Montoya-Contreras A, Bautista-Perez R, Martinez-Morales F: Autocrine modulation of glucose transporter SGLT2 by IL-6 and TNF- α in LLC-PK1cells. *J Physiol Biochem* 2012;68:411-420.
- 45 Patel H, Chen J, Das KC, Kavdia M: Hyperglycemia induces differential change in oxidative stress at gene expression and functional levels in HUVEC and HMVEC. *Cardiovasc Diabetol* 2013;12:1-14.

- 46 Azcutia V, Abu-Taha M, Romacho T, Vázquez-Bella M, Matesanz N, Luscinskas FW, Rodríguez-Mañas L, Sanz MJ, Sánchez-Ferrer CF, Peiró C: Inflammation determines the pro-adhesive properties of high extracellular D-glucose in human endothelial cells *in vitro* and rat microvessels *in vivo*. PLoS One 2010;5:e10091.
- 47 Zhu M, Wen M, Sun X, Chen W, Chen J, Miao C: Propofol Protects Against High Glucose-Induced Endothelial Apoptosis and Dysfunction in Human Umbilical Vein Endothelial Cells. Anesth Analg 2015;120:781-789.
- 48 Endo S, Inada K, Yamada Y, Kasai T, Takakuwa T, Nakae H, Kikuchi M, Hoshi S, Suzuki M, Yamashita H: Plasma tumour necrosis factor- α (TNF- α) levels in patients with burns. Burns 1993;19:124-127.
- 49 Zhao SP, Zeng LH: Elevated plasma levels of tumor necrosis factor in chronic heart failure with cachexia. Int J Cardiol 1997;58:257-261.